BJPS

Brazilian Journal of
Pharmaceutical Sciences

http://dx.doi.org/10.1590/s2175-97902023e21114

Article

Mechanical, optical, and physicochemical properties of HPMC-based doxazosin mesylate orodispersible films

Pamela Coradi da Silva[1], Larissa Aroca Colucci[2], Larissa Lea da Silva[3], Celso Molina[1], Marcelo Dutra Duque[3], Leticia Norma Carpentieri Rodrigues[3*]

[1]Department of Chemistry, Federal University of São Paulo, Diadema, SP, Brazil, [2]Methodist University of São Paulo, 09641-000, São Bernardo do Campo, SP, Brazil, [3]Department of Pharmaceutical Sciences, Federal University of São Paulo, Diadema, SP, Brazil

In this study, orodispersible films formed from hydroxypropyl methylcellulose (HPMC) E6 (2, 2.5, and 3%) and plasticizers ((glycerin (Gly), propylene glycol (PP), or polyethylene glycol (PEG)), containing doxazosin mesylate, were prepared by the solvent casting method and characterized. Design of experiments (DoE) was used as a statistical tool to facilitate the interpretation of the experimental data and allow the identification of optimal levels of factors for maximum formulation performance. Differential scanning calorimetry (DSC) curves and X-ray powder diffraction (XRPD) diffractograms showed doxazosin mesylate amorphization, probably due to complexation with the polymer (HPMC E6), and the glass transition temperature of the polymer was reduced by adding a plasticizer. Fourier transformed infrared (FTIR) spectroscopy results showed that the chemical structure of doxazosin mesylate was preserved when introduced into the polymer matrix, and the plasticizers, glycerin and PEG, affected the polymer matrix with high intensity. The addition of plasticizers increased the elongation at break and adhesiveness (Gly > PEG > PP), confirming the greater plasticizer effect of Gly observed in DSC and FTIR studies. Greater transparency was observed for the orodispersible films prepared using PP. The addition of citric acid as a pH modifier was fundamental for the release of doxazosin mesylate, and the desirability formulation had a release profile similar to that of the reference product.

Keywords: Orodispersible films. Design of experiments. Doxazosin mesylate. FTIR. Mechanical properties. Desirability function.

INTRODUCTION

Researchers worldwide are trying to explore orodispersible films as a new strategy for drug release, especially for patients at risk of choking and facing impediments to oral administration, as well as pediatric, geriatric, and psychiatric patients (Preis, Knop, Breitkreutz, 2014; Karki *et al*., 2016; Musazzi *et al*., 2020).

Orodispersible films are ultrathin, with 50–150 µm thickness and 1–20 cm^2 of surface area, which disintegrate quickly or dissolve within one minute of contact with saliva, resulting in increased bioavailability and fast absorption, reducing the exposure of the substances to degradation in the gastrointestinal tract, and pre-systemic metabolism (Chonkar, Bhagawati, Udupa, 2015; Karki *et al*., 2016). Orodispersible films are normally composed of a water-soluble polymeric matrix, which once administered in the oral cavity, undergoes hydration, adhering, and disintegration. Absorption of the active pharmaceutical ingredients (APIs) in this dosage form can occur in the oral mucosa (gingival, sublingual, buccal, and palatal regions) and also in the gastrointestinal tract (Borges *et al*., 2015). Regardless of the route involved in the absorption process, orodispersible films are associated with increased bioavailability of APIs compared to conventional oral solid dosage forms, because the release occurs in the oral cavity and the dissolution of the API begins earlier. The surface area of the human oral mucosa of an adult individual is 215 cm^2, and most of the tissue is not keratinized, presenting high permeability, which, combined with the high rate of

***Correspondence:** L. N. Carpentieri-Rodrigues. Departamento de Ciências Farmacêuticas. Universidade Federal de São Paulo. Rua São Nicolau, 210, 09913-030, Diadema, SP, Brasil. Phone: +55 11 4044-0500. VoIP 3576. E-mail: leticia.carpentieri@unifesp.br. ORCID: https://orcid.org/0000-0001-5175-859X

blood flow, enables rapid systemic reach, reducing the effect of the first hepatic passage (Preis, Knop, Breitkreutz, 2014; Siddiqui, Garg, Sharma, 2011). The major limitation of orodispersible films is their limited drug loading capacity, and thus, the restriction of drugs employed in high doses (Dixit, Puthli 2009; Musazzi *et al*., 2020).

Hydrodispersible polymers are the main components of orodispersible films (Chonkar, Bhagawati, Udupa, 2015; Chauhan, Solanki, Sharma, 2018). According to Mahadevaiah *et al.* (2017), the addition of a plasticizer is fundamental to reducing the fragility and increasing the flexibility of films. Hydroxypropyl methylcellulose (HPMC) is a water-soluble polymer formed by cellulose monomer ethers, which are non-ionic, biodegradable, pH 3–11, stable, and have good film-forming properties (Dixit, Puthli 2009; Morales, McConville 2011; Rani *et al*., 2013; Rowe, Sheskey, Quinn, 2015).

Quinazolines and their derivatives exhibit a diverse range of biological activities. Doxazosin mesylate (DOX) is a quinazoline, a selective α_1-adrenergic receptor blocker, used for the treatment of hypertension and benign prostatic hyperplasia. Recent studies have shown its neuroprotective effects in neurodegenerative diseases, such as Alzheimer's disease (Coelho *et al.,* 2019). DOX is a weak base salt (pk_{a1} = 12,67 e pk_{a2} = 7,24) and its bioavailability (63%) is strongly dependent on pH (Cha *et al*., 2010). Its metabolism in humans mainly involves o-demethylation of quinazoline substituents or hydroxylation of the benzdioxan moiety. The high half-life of DOX (~9-11.5 h) favors its administration in daily single oral doses (Vincent *et al*., 1983; Faulkner *et al*., 1987; Altiokka, 2001). The therapeutic dose of DOX is 1–16 mg daily and is available in the form of oral tablets for immediate and prolonged release.

Oral films are intended to deliver drugs via the oral mucosa. Therefore, oral mucosa drug saturation should be considered, as saliva plays a critical role in the absorption of drugs in these dosage forms. Among the parameters that may have an impact on the dissolution of drugs, the pH (6.97–7.40), viscosity (1.5–1.6 mPa s), and salivary flow (0.58–1.51) must be considered (Borges *et al*., 2015; Gittings *et al*., 2015).

There is an increasing number of published studies on the application of statistically based optimization processes in the field of pharmaceutical technology. Design of experiments (DoE) is a statistical tool capable of facilitating the interpretation of experimental data, which ultimately allows the identification of optimal factor levels for maximum performance (Uhoraningoga *et al*., 2018; Barthi, Mittal, Mishra, 2019).

Since DOX is a weakly basic salt and its solubility and bioavailability are pH-dependent, oradispersible films can be a good alternative to oral administration of DOX for continuous use and emergency situations.

In this study, HPMC-based orodispersible films containing DOX were developed and characterized using a DoE approach to evaluate the effects of the formulation components on their physical, chemical, and release characteristics.

MATERIAL AND METHODS

Material

DOX (99.74% purity) was kindly provided by EMS Pharma (Hortolandia, São Paulo, Brazil). HPMC E6 (Premium LV; Dow Chemical Company, Latin America) was kindly provided by Colorcon Inc. (Cotia, Brazil), glycerin (Gly), propylene glycol (PP), polyethylene glycol (PEG)-400, and citric acid monohydrate were obtained from LabSynth (Diadema, Brazil). Tablets containing 2.43 mg of DOX (Cardura™ 2 mg tablets; Pfizer Inc., Brazil) were obtained from the pharmaceutical market. Purified water was obtained using a reverse osmosis system Gehaka model OS10LXE (São Paulo, Brazil).

Preparation of orodispersible films

Orodispersible films were prepared using a full factorial DoE approach employing two factors and three levels (3^2) using the Statistica version 13.1 software (TIBCO Statistica Inc., CA, USA), resulting in nine formulations. The films were prepared by the solvent casting method using HPMC E6 (2, 2.5, and 3%) as a film-forming agent, and GLY, PP, or PEG as plasticizers (10% mass polymer, w/w) (Table I) (Dixit, Puthli, 2009; Musazzi *et al*., 2020).

TABLE I - Composition of orodispersible films according to the design of experiments (DoE)

Components	F3	F9	F5	F2	F1	F8	F7	F4	F6
DOX (mg)	2.43	2.43	2.43	2.43	2.43	2.43	2.43	2.43	2.43
Plasticizer[a]	PEG	PEG	PP	PP	GLY	PP	GLY	GLY	PEG
HPMC E6 (%)	2	3	2.5	2	2	3	3	2.5	2.5
Purified water, qsp	6	6	6	6	6	6	6	6	6

[a]*10% mass polymer, w/w*

To prepare the formulations 2.4 mg of DOX, 2.0 mg of doxazosin base was weighed, dispersed in sufficient amount of purified water, and subjected to stirring on a 10-position magnetic stirrer. Then, the plasticizer (GLY, PP, or PEG) and HPMC E6 (2, 2.5, or 3%) were added, and the volume was completed with purified water (q.s. to 6 mL). After 30 min, stirring was stopped, and the dispersions were kept at rest for 30 min for deaeration (Karki *et al.*, 2016). The dispersions thus obtained were transferred to a polyethylene mold containing 12 circular cavities, each 50 mm in diameter, and dried in an oven with forced air circulation and renewal (40.0 ± 0.5 °C) for 24 h. The films were removed from the molds, wrapped in an aluminum foil, and placed in a desiccator.

Characterization and optimization

Thermal analysis

DOX, HPMC E6, physical-mixture DOX:HPMC E6 1:1 (w/w) (PM), and orodispersible films (F1-9) were evaluated using differential scanning calorimetry (DSC) (~2–4 mg) and thermogravimetric analysis (TGA) (~4–8 mg).

DSC curves were obtained using a DSC Shimadzu model DSC-60 at a heating rate of 10 °C min^{-1} over a temperature range of 40–600 °C. Samples of 2–4 mg were used in sealed aluminum pans under a dynamic nitrogen atmosphere (100 mL min^{-1}). The system was previously calibrated with metallic indium (99.99% purity, $T_{melting}$ = 156.4 °C, $\Delta H_{melting}$ = 28.7 J g^{1}.

TGA curves were obtained using a TGA Shimadzu model DTG-60 at a heating rate of 20°C min^{-1} over a temperature range of 40–900 °C. Sample (5–7 mg) was used in a platinum pan under a dynamic nitrogen atmosphere (100 mL min^{1}). System calibration was performed using a calcium oxalate monohydrate standard. The curves were analysed using the TA-60WS software.

Fourier transformed infrared (FTIR) spectroscopy

Absorption spectra of DOX, HPMC E6, orodispersible films with a plasticizer (F1-9), and without a plasticizer (WP-F1, WP-F4, and WP-F7) were obtained using an infrared spectrophotometer (FTIR Shimadzu model IR, Prestige-21) coupled with a total attenuated reflection (ATR) accessory, with a resolution of 4 cm^{-1} over the full spectral range (4000–400 cm^{-1}).

X-ray powder diffraction (XRPD)

X-ray powder diffraction patterns of DOX, HPMC E6, orodispersible films with the plasticizer (F1-9), and without plasticizer (WP-F1, WP-F4, and WP-F7) were obtained using a diffractometer (Bruker D8 Advance X-ray powder diffractometer) employing a radiation source Cu K_{α} operating at 40 kV, 40 mA, scan range from 5–60° (2 theta), and scan rate of 2 °C min^{-1}. Polycrystalline silicon (Si) was used as the standard.

Physical and mechanical properties

The thickness of the orodispersible films was measured in continuous mode using a Defelsko Inspection Instruments model PosiTector Standard 200 (ASTM D-6132-13) with an accuracy of 0.001 ± 0.0001 µm.

The mechanical properties of the orodispersible films were evaluated using a puncture (ASTM D2582-16) and pull-off adhesion (ASTM D4541-17) tests, using a Brookfield CT3 Texture Analyser with a 50 kg load cell. The tests were performed using the Texture ProCT software.

For the puncture test, the samples were fixed in the TA-FSF accessory, placed on the TA-BT-kit (fixture base table), and subjected to puncture strength using a TA39 probe (2 mm D, 200 mm L, stainless steel). Load *vs.* displacement data were recorded from the point of contact of the probe with the film until the film ruptured. The puncture strength, elongation at break, and puncture to energy were calculated according to the method described by Radebaugh *et al.* (1988). The nature of the test did not allow the calculation of Young's modulus (Radebaugh *et al*., 1988; Karki *et al*., 2016).

In the adhesion test, an epithelium segment of the pig oral mucosa (Animal Ethics Committee n° 1352120520) was fixed on the mucus adhesion text fixture (TA-MA) accessory, submitted in a borosilicate glass flask containing 0.9% physiological solution to reach the lower surface of the mucosa, with stirring at 37.5 °C. On the probe TA5 (12.7 mm D, 35 mm L; Black Delrin), a piece of double-sided adhesive tape was applied, and the sample was deposited on it. The parameters of hardness, adhesive force, and adhesiveness were evaluated (Carvalho *et al.,* 2010).

Optical properties

Color determination of the orodispersible films was carried out using a CR-400 colorimeter (Konica-Minolta, Co. Ltd., Japan) calibrated with black and white backing, using standard D65 illumination and a 10° absorber. The tests were performed in triplicates.

The CIELAB reading system was represented by coordinate *L* C*h*, where *L** (lighntness) (0=black,and 100=white), *C** (Chromaticity), and h (tone angle) (-a*=0°,green; +b*=90°,yellow; +a*=180°,red; and -b*=270°, blue). The opacity of the samples was calculated on the same colorimeter by coordinates Yxy using the following equation: $Y(\%)= Y_b/Y_w$ x 100, where Y is the opacity (%), Y_b is the opacity of the sample on the black backing, and Y_w is the opacity of the white backing (Santana *et al.,* 2018).

Scanning electron microscopy (SEM) analysis

The morphology of the orodispersible films was evaluated using SEM JEOL model JSM-6610. The samples were fixed on a metallic support with the aid of a 12 mm thick double-sided carbon tape and subjected to metallization under vacuum to make them electrically conductive. The visualization was performed with an increase of 1.000 × with an excitation voltage of 10–15 kV.

Content uniformity

Orodispersible films were transferred to Falcon 15 mL conical tubes, 5 mL of purified water was added, stirred on a vortex-type agitator for 60 s, and filtered through filter paper. Aliquots of 100 µL were diluted 1:100 (v/v) and quantified using a Thermo Scientific spectrophotometer (Evolution 200) at 246 nm. The final values are the averages of three measurements.

Dissolution profile

Dissolution profiles were obtained using the dissolution equipment Ethik Technology model 299/TTS. A total of three units of each dosage forms (orodispersible films, or reference product, Cardura™ 2 mg tablets; Pfizer Inc., Brazil) containing 2.43 mg of DOX (equivalent to 2.0 mg doxazosin base) were subjected to the dissolution tests using the following conditions:

Orodispersible films: Apparatus 5 (paddle over disc), stirring speed 50 rpm, medium volume 500 mL, UV spectrophotometry at 246 nm, and phosphate buffer pH 7.4 at 37 ± 0.5 °C as dissolution medium (Krampe *et al.*, 2016).

Reference product, Cardura™ 2 mg tablets: Apparatus 2 (paddle) stirring speed 50 rpm, medium volume 500 mL, UV spectrophotometry at 246 nm, and

hydrogen chloride (HCl) 0.01 M at 37 ± 0.5 °C dissolution medium (USP, 2015).

The dissolution efficiency (DE) was obtained from the average dissolution profile for each formulation according to the equation (Simionato *et al.*, 2018) $DE\% = [\int_0^T (y\ x\ dt)/y_{100}\ x\ (t_t - t_0)]\ x\ 100$ where y_t is percent of drug dissolved at any time t, y_{100} denotes 100% dissolution, and the integral represents the area under dissolution curve between time zero and T.

The model-independent approach employing the difference factor(f_1) and similarity factor (f_2) was used to compare the dissolution profiles. According to this approach, f_1 values up to 15 (0–15), and f_2 values greater than 50 (50–100) ensure sameness or equivalence of the two curves (Xie, Ji, Cheng, 2015).

pH and water activity (A_w)

Orodispersible films were transferred separately to Falcon (15 mL) conical tubes, where 5 mL of purified water was added, and evaluated using a pH meter (Hanna model pH21) with Ag/AgCl electrode.

A_w was evaluated using the FA-st Water Activity Meter (GBX Instruments, France) previously calibrated with k_2SO_4 ($A_w = 0.970 \pm 0.003$) (at room temperature. The final values are the averages of three measurements.

Data processing

Statistica version 13.1 software (TIBCO Software Inc., CA, USA) was used for the statistical analysis of the data. The results of thickness, mechanical properties, opacity, and dissolution efficiency were analyzed using DoE for the models without interaction, and with two-level interactions, (linear, linear) or (linear, quadratic). The desirability method was used to optimize the formulations (Candioti *et al.*, 2014). Principal component analysis (PCA) and hierarchical cluster analysis were used to explain the optical properties of CIE-*LCh*.

RESULTS AND DISCUSSION

Thermal analysis

The thermal properties of DOX, HPMC E6, and orodispersible films were evaluated using DSC and TGA (Table II).

TABLE II - Data obtained for doxazosin mesylate (DOX), hydroxypropyl methylcellulose (HPMC) E6, physical-mixture 1:1 (w/w) (PM), and orodispersible films (F1-9) from (TGA) and differential scanning calorimetry (DSC) curves

	DSC			TGA		
	(°C)	(°C)	(J g^{-1})	(°C)	%	%
DOX	278.23		93.62	292.05/343.37	0.29	31.55/27.09
HPMC E6	-	177.0	-	251.60	2.96	86.88
PM	254.81		132.62	241.96/283.29	0.82	33.23/19.50
F1		162.0		246.27/377.70	3.12	70.62/23.20
F2		168.6		231.65	0.95	96.32
F3		163.8		238.38	0.46	92.84
F4		154.9		250.31	20.63	72.12
F5		163.8		243.58/399.94	11.10	40.12/38.83
F6		165.8		261.09	2.35	90.93
F7		154.0		263.34	20.46	75.93
F8		164.1		241.17	3.76	86.98
F9		164.2		266.11	3.46	87.12

[a]*T melting,* [b]*glass transition temperature,* [c]*enthalpy, and* [d]*weigth loss*

The DSC curve of DOX showed an endothermic event at 278.23°C ($\Delta H = 93.62$ J g^{-1}) relative to the melting of the drug, followed by exothermic decomposition at this temperature. The TG/DTG curves of DOX indicate that the crystalline form is thermally stable up to 292.05°C and thermal decomposition occurs in two events. The first event occurred with fast kinetics between 292.05°C and 343.37 °C, with a mass loss of approximately 31.55%; the second event occurred more slowly and gradually between 343.37 and 520.75 °C, and the mass loss is approximately 27.09%; a residual content of approximately 12.03%. The predominantly exothermic events observed in the DSC curves are concordant with those of the mass loss observed in the TG/DTG curves.

Grčman, Vrečer and Meden (2002) described several polymorfic modifications of DOX, designed as A, D, E, F, G, H, and I. The T_m of DOX obtained suggests a polymorph A-like considering T_m at 277.9 ± 0.2 °C or a polymorph F-like (Tm at 276.5 ± 0.2 °C), which presents X-ray powder diffraction patterns that are more similar when compared with DOX in the present work. A polymorph with lower solubility is the more thermodynamically stable form.

XRPD, owing to its absolute specificity, is widely recognized as the gold standard for the identification and quantification of crystalline forms. Every crystalline form has a unique XRPD pattern, which is unaffected by other constituents in the formulation. However, most APIs are organic compounds, and their crystal structures are characterized by large unit cells with low symmetry. The utility of conventional XRPD equipment in the characterization of such compounds is often limited by the appearance of numerous overlapping peaks with low intensities, posing challenges with respect to both resolution and sensitivity. The sensitivity is also limited by the low flux of the X-ray source (usually a sealed tub) (Munjal, Suryanarayanan 2021). In parallel, it is already known that thermograms can differ depending on the application of different parameters, for example, heating rates and amount of sample (Dedroog *et al*., 2020). Therefore, one should keep the limitations of each assay in mind to avoid misinterpretation.

The DSC curve of HPMC E6 remained stable up to 291.29 °C with exothermic degradation at this temperature. The glass transition temperature (T_g) of HPMC E6 was 177.0°C. The TG/DTG curves of HPMC E6 showed an endothermic event at a temperature below 100°C, referring to dehydration ($\Delta m_1 = 2.96\%$) followed by single-stage decomposition between 251.60 and 404.23°C ($DTG_{peak} = 358.99$°C, $\Delta m_2 = 86.88\%$) with carbonization and elimination of the carbonaceous material from 400 °C ($\Delta m_2 = 8.00\%$).

A decrease in the DOX melting point was observed for the physical-mixture 1:1 (w/w) (PM), suggesting the occurrence of some interaction between the drug and the polymer (Ramaraj, Nayak, Yoon, 2010). In the TG/DTG curves of the physical mixture, the thermal events correspond to the sum of the effects observed in the thermograms of the individual components.

In DSC curves of the orodispersible films, the event related to DOX melting was suppressed, supposedly due to conversion into its amorphous form (Dinge, Nagarsenker 2008; Siddiqui Garg, Sharma, 2011). The TG/DTG curves of the orodispersible films showed decomposition in a single step; the TG/DTG curves of the F1 and F2 films showed two-step decomposition, similar to that of the physical mixture, probably due to the inhomogeneity of the samples (Table II).

The formation of amorphous solid dispersions (ASDs), in which API is dispersed in a polymer matrix, thus forming an amorphous one-phase system, is one of the main strategies employed in the pharmaceutical industry to increase the solubility and stability of drugs (Dedroog *et al*., 2020). Water-soluble polymers can interact with drug molecules through ion-ion, ion-dipole, and dipole-dipole electrostatic bonds, van der Waals forces, and hydrogen bonds, resulting in polymer-(drug)n complexes (Veiga *et al*., 2006). According to Usui *et al.* (1997), the increased stability in dispersed systems can be attributed not only to the increased viscosity of the systems, but also to the establishment of interactions between the components.

The glass transition temperature (T_g) (corresponds to the temperature at which the polymer changes from a state of relative molecular stiffness (glass phase) to considerable chain mobility (rubber phase), where the efficiency of the plasticizer is proportional to the lowering of the T_g (Mahadevaiah *et al*., 2017). The incorporation of a plasticizer (Gly, PP, or PEG) reduced the glass transition

temperature of HPMC E6 in the orodispersible films (Table II) (Dixit et al., 2009).

FTIR spectroscopy

Figure 1 (**a-e**), panel A, shows the FTIR spectra of DOX, HPMC E6, and orodispersible films without plasticizer (WP-F1, WP-F4, and WP-F7). The main bands of DOX are assigned to tertiary amide ν(C=O) at 1634 cm^{-1} (1); to δ(N-H) aromatic at 1595 cm^{-1} (2); to ν(C=N) at 1494 cm^{-1} (3); to ν(C-N) aromatic amine at 1265 cm^{-1} (4); to ν(C-O) of cyclic ether at 1113 cm^{-1} and 1043 cm^{-1} (5)(6) (Pupe *et al.*, 2013; Biswas *et al.*, 2015; Khalilullah *et al.*, 2016). Figure 1b, panel (A) shows the most important vibrational band of the HPMC E6 observed as broadband with maximum absorption at 1064 cm^{-1} (7), and a shoulder at 1115 cm^{-1} attributed to ether type ν(C-O) (Van Der Weerd, Kazarian, 2004; Wray, Clarke, Kazarian, 2011; Hazzah *et al.*, 2013). The presence of DOX as a function of HPMC E6 content is given in (Figure 1 (c-e), Panel A). It is clear from the results presented here that the attributed bands depicted as (1-4) confirm the presence of the drug dispersed in the polymeric matrix and indicates that its structure was preserved.

Figure 1 (**c-e**), panel (B), presents the effect of the inclusion of plasticizers in orodispersible films: F1 (glycerin, Gly), F2 (propylene glycol, PP), and F3 (polyethylene glycol 400, PEG). The main features observed were the low intensities of DOX bands (2) and (3), and some other bands overlapped on the HPMC E6 bands. Moreover, the bands practically remained unaffected by the inclusion of PP plasticizer (Figure 1**c**) panel B. This behavior can be attributed to the low interaction between PP, and polymer matrix. On the other hand, changes were detected in the FTIR spectra of F1, and F3 (Figure 1 (**d-e**), panel B). In the presence of Gly (Figure 1**d**, panel B), the ν(C-O) (7) was shifted 21 cm^{-1}, and appeared at 1043 cm^{-1}, suggesting that strong interaction occurred. Besides, a slight shift also was observed to PEG plasticizer with a broadening of this band, and an appearance of a shoulder with a maximum at 1096 cm^{-1} (Figure 1**e**, panel B). The DOX bands appeared with low intensity being more pronounced to PEG plasticizer. The intermediate and high concentrations of HPMC indicated that no effective influence of plasticizer occurred (Figure 1, Panel C and D). Additionally, bands of DOX were more pronounced to PEG to F6 (Figure 1**e**, Panel C), and Gly to F7 (Figure 1**d**, Panel D), respectively.

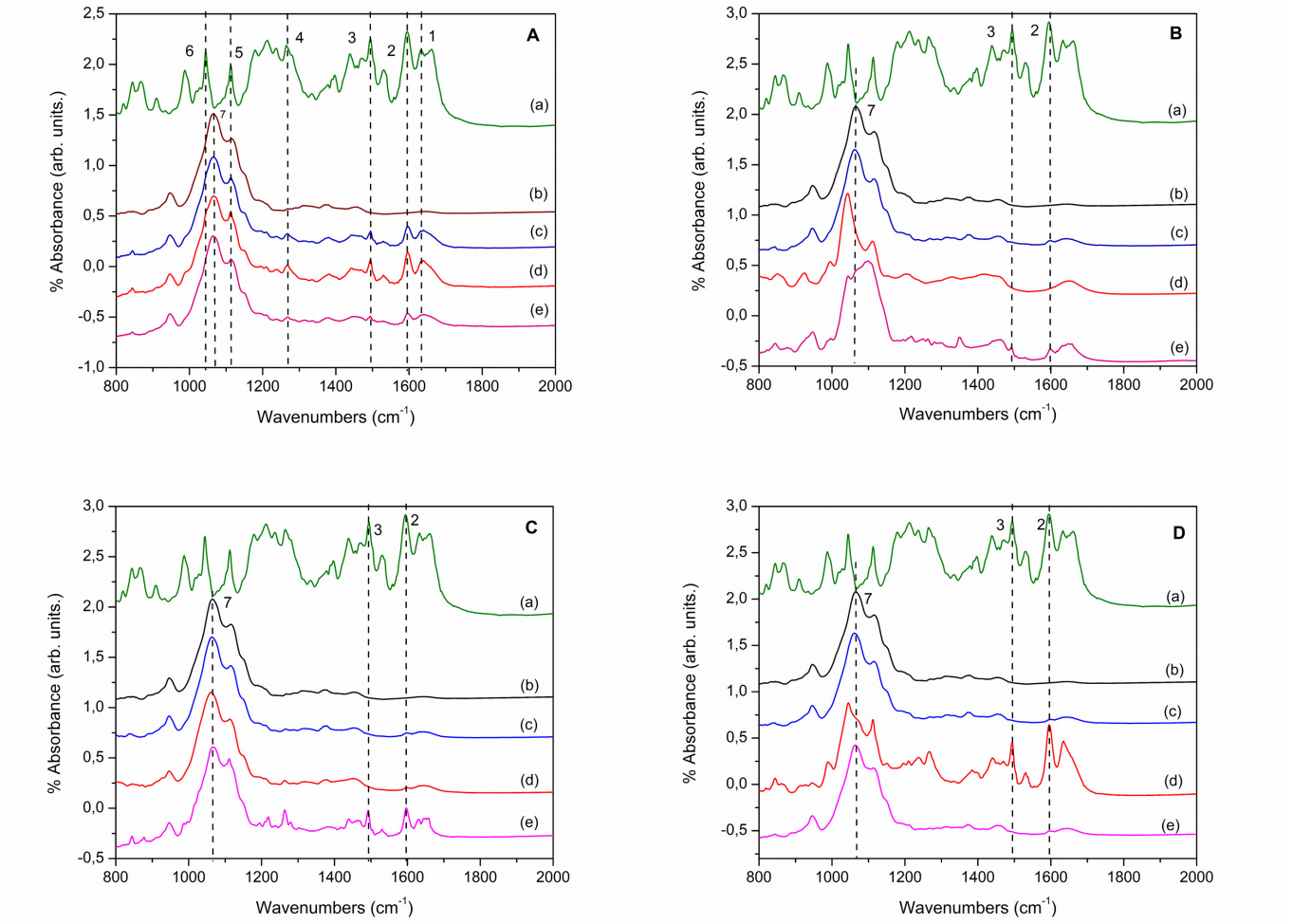

FIGURE 1 - Fourier transformed infrared (FTIR) spectra of panel (A): doxazosin mesylate (DOX) (a), hydroxypropyl methylcellulose (HPMC) E6 (b), without plasticizer (WP)-F1 (c), WP-F4 (d), and WP-F7 (e); panel (B): DOX (a), HPMC E6 (b), F2 (c), F1 (d), and F3 (e); panel (C): DOX (a), HPMC E6 (b), F5 (c), F4 (d), and F6 (e); and panel (D): DOX (a), HPMC E6 (b), F8 (c)d F7 (d), and F9 (e).

XRPD

Figure 2 (**a-n**) show powder X-ray powder diffraction patterns of DOX, HPMC E6, and orodispersible films (F1-9). The X-ray powder diffraction patterns of DOX (Fig. 2**a**) presented sharp peaks (16.8°, 17.1°, 18.2°, and 24.05°, 2θ) indicating the crystalline structure of the drug (Grčman, Vrečer, Meden, 2002; Pupe *et al.*, 2013). The HPMC E6 cellulose derivative presented a characteristic semi-crystalline structure (Figure 2b), revealing two main broad peaks at approximately 9.14° and 19.5° (2θ) (dashed lines), and three very low-intensity sharp peaks (*) at 27.3°, 31.6°, and 45.4°, respectively. Figure 2 (**c-e**) depicts the effect of the DOX inclusion as a function of the HPMC content from 2% to 3%. It was possible to observe that sharp peaks of DOX disappeared indicating that the drug when introduced in the HPMC matrix the "amorphous" halo profile remains. Moreover, the extremely low-intensity sharp peaks of the polymer matrix (HPMC E6) also disappeared, leading to an enhancement of the amorphous state. Furthermore, the broad peaks were slightly shifted in two θ values, suggesting that changes in the local distance occurred. Taking into account the introduction of plasticizers PP, Gly, or PEG as a function of HPMC E6 content, amorphous behavior was observed without any significant changes for all compositions (Figure 2 (**f –n**)).

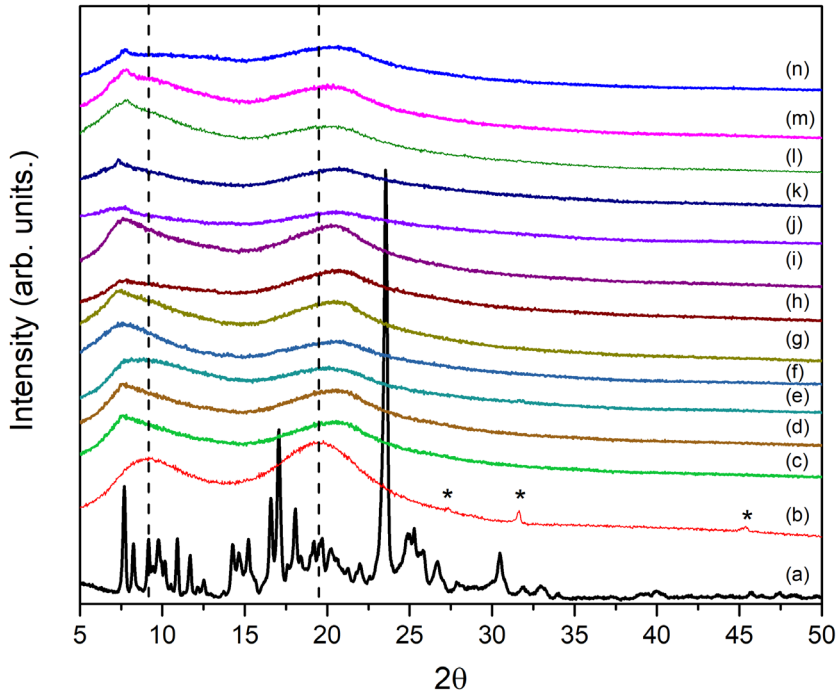

FIGURE 2 - X-ray powder diffraction patterns of DOX (a), HPMC E6 (b), WP-F1 (c), WP-F4 (d), WP-F7 (e), F1 (f), F2 (g), F3 (h), F4 (i), F5 (j), F6 (k), F7 (l), F8 (m), and F9 (n).

Amorphous solid dispersions (ASDs) are single-phase amorphous systems in which drug molecules are molecularly dispersed (dissolved) in a polymer matrix. Dedroog *et al.* (2020) studied the techniques of (modulated) DSC and XRPD to elucidate the phase behavior of ASDs and concluded that both techniques, although widely used for this purpose, have limitations. According to the authors, the limiting factors of XRPD were the lack of sensitivity for small traces of crystallinity, the inability to differentiate between distinct amorphous phases, and the impossibility of detecting nanocrystals in a polymer matrix. In addition, the limiting factors of (m)DSC were the heat-induced sample alteration upon heating, the interference of residual solvent evaporation with other thermal events, and the coincidence of enthalpy recovery with melting events.

Physical and mechanical properties

The thickness values (Table III) obtained agree with the ideal values described in the literature (Karki *et al.*, 2016). For the thickness parameter, the two-level interaction model (linear, linear) was the most appropriate (R-sqr = 0.98648; Adj:0.96395), and only the variable polymer (linear) showed a significant effect ($p < 0.05$), such that the thickness of the orodispersible films increased as a function of the amount of HPMC E6 present in the formulation (Figure 3).

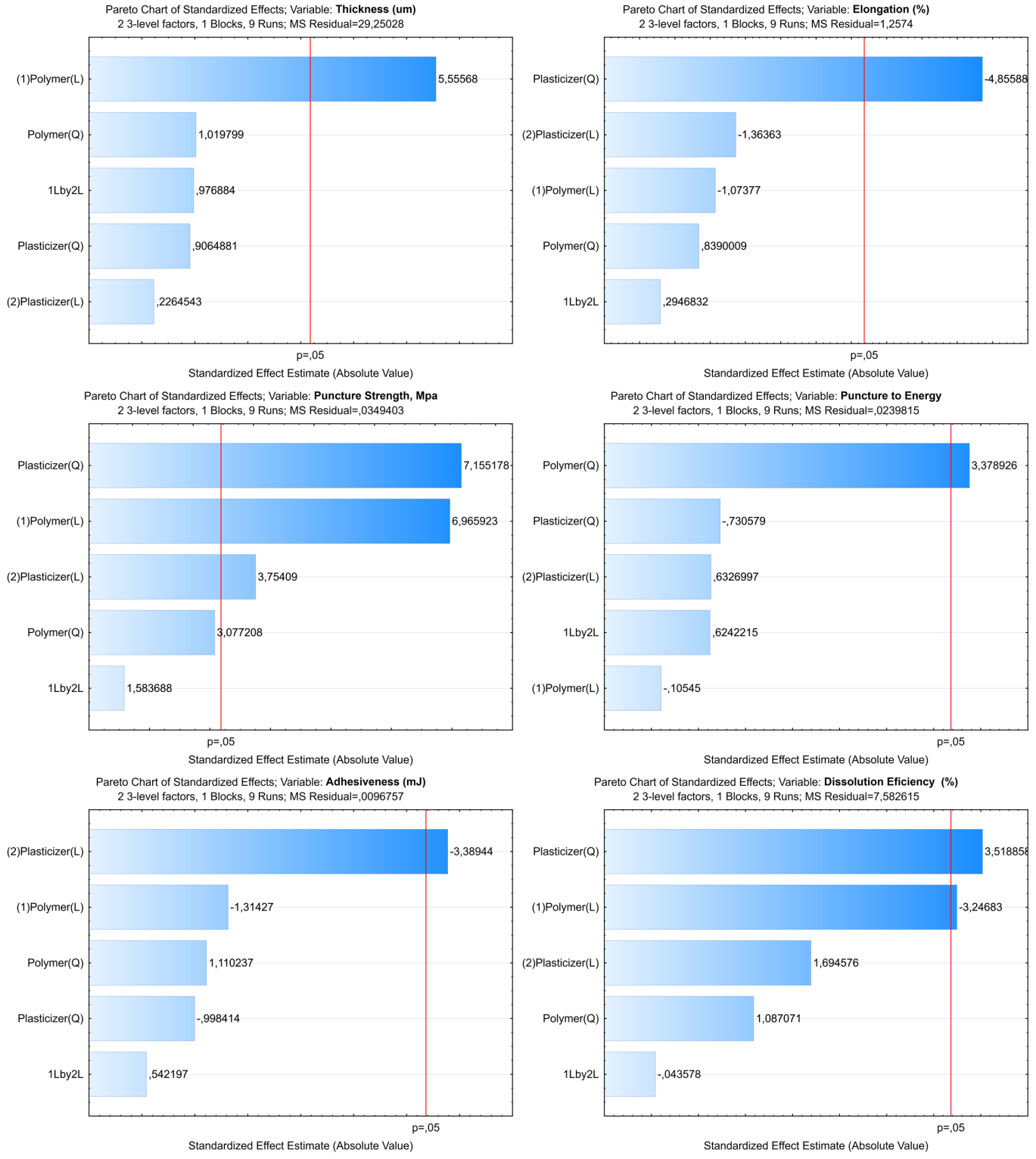

FIGURE 3 - Pareto chart of the main effects of variables (polymers and plasticizers) on the investigated responses

TABLE III - Average values (n = 3) of the physicochemical and mechanical properties of orodispersible films

Parameters*	Orodispersible films								
	F1	F2	F3	F4	F5	F6	F7	F8	F9
Thickness, μm	54.53±0.47	54.73±1.67	54.80±3.82	74.27±1.93	72.13±4.09	66.17±1.19	84.33±4.72	84.83±3.09	81.83±1.35
$pH_{5\%}$	5.42±0.04	5.54±0.13	5.54±0.11	5.55±0.01	5.48±0.03	5.59±0.10	5.65±0.08	5.60±0.07	5.61±0.10
A_w	0.80±0.00	0.80±0.01	0.77±0.01	0.78±0.01	0.76±0.01	0.74±0.02	0.78±0.00	0.78±0.01	0.73±0.00
UC, mg	2.36±0.06	2.42±0.02	2.43±0.02	2.48±0.12	2.36±0.03	2.42±0.02	2.39±0.03	2.48±0.13	2.40±0.02
Opacity, %	15±0.00	13±0.01	24±0.05	13±0.01	14±0.01	22±0.01	12±0.02	13±0.01	18±0.01
DE, %	80.86±0.01	86.89±0.02	83.86±0.02	77.94±0.02	85.46±0.10	83.61±0.06	71.41±0.05	84.13±0.11	74.17±0.03
Puncture test									
E, %	9.52±0.03	4.11±0.01	8.35±0.02	10.10±0.02	4.38±0.00	8.03±0.01	7.28±0.01	4.98±0.01	6.77±0.01
PS, Mpa	1.60±0.56	2.46±0.38	1.74±0.31	2.06±0.40	3.64±0.18	2.90±0.19	2.33±0.47	3.59±0.43	3.06±0.50
PE, N/mm^3	1.01±0.15	1.06±0.09	1.09±0.16	1.57±0.80	1.22±0.12	1.46±0.11	0.89±0.14	1.07±0.15	1.16±0.27
Adhesiveness test									
Hardness, N	16.97±3.51	31.50±1.66	23.52±2.16	15.11±2.11	24.03±1.77	19.48±1.41	15.06±2.08	23.37±4.26	18.22±4,56
AF, N	0.15±0.00	0.28±0.19	0.28±0.11	0.33±0.10	0.31±0.08	0.18±0.04	0.28±0.11	0.23±0.12	0.19±0.07
Adhesiveness, mJ	0.52±0.12	0.16±0.08	0.23±0.25	0.48±0.47	0.37±0.13	0.14±0.04	0.31±0.27	0.16±0.10	0.13±0.09

*Mean ± standard deviation; Water activity; UC, Uniformity content; DE, Dissolution efficiency;E, Elongation at break; PS, Puncture strength; PE, Puncture to energy; and, AF, Adhesive force.

In the industrial process, the production of films based only on polymers is inconvenient because their mechanical properties make it difficult to extrude them into molds. Plasticizers are molecules with low molecular weight and low volatility, which reduce intermolecular interactions by coupling between the polymer chains, increasing their mobility and reducing the glass transition temperature, viscosity, Young's modulus, and fragility of the films (Santana *et al*., 2018).

Traditionally, stress-strain testing is the most popular and widely used mechanical test for pharmaceutical films; however, it has limitations (Preis, Knop, Breitkreutz, 2014). Tension-strain testing is designed for tough materials, and therefore has limited sensitivity for polymers (Radebaugh *et al*., 1988); in parallel, and the sample size required for clamping between grips in tension-strain testing (100 × 25.4 mm) often becomes inconvenient owing to the difficulty and high cost of developing films of these dimensions (Preis, Knop, Breitkreutz, 2014). The puncture test consists of an alternative method to evaluate the mechanical properties of oral films capable of overcoming these disadvantages (Karki *et al*., 2016).

In the puncture test, the two-level interaction model (linear, linear) was the most appropriate for all parameters evaluated (Table III, Figure 4). For parameter puncture strength (R-sqr = 0.97671; Adj: 0.93788), the variables–polymer (linear), and plasticizer (linear, quadratic)–had a significant influence ($p < 0.05$), as the puncture strength increased with polymer concentration, and the effect of plasticizer obeyed the following order: PP>PEG>GLY; for the parameter elongation at break (R-sqr = 0.90126; Adj: 0.73669), the variable plasticizer (quadratic) presented a significant influence ($p < 0.05$), and varied in the following order: Gly>PEG>PP; and finally, for the parameter puncture to energy (R-sqr = 0.80955; Adj: 0.49213), only

the variable polymer (quadratic) presented a significant influence ($p < 0.05$), where greater puncture to energy was observed when 2.5% of the polymer was used.

Puncture strength is a measure of toughness and is directly proportional to the resistance to break or fracture. Toughness is quantified as energy (Radebaugh *et al*., 1988). Puncture strength is a measure of the intensity of interatomic bond forces, and the addition of plasticizers causes a reduction in the puncture strength, regardless of the plasticizer type. Plasticizers decrease the molecular attraction between adjacent polymer chains, increase the mobility between molecules, decrease the glass transition temperature, and improve polymer flexibility and elasticity (Mahadevaiah *et al.,* 2017). The physical and chemical properties of the plasticizer, such as its chemical structure, shape, polarity, chain length, physical state, and the number of active functional groups, determine its ability to plasticize a polymer network (Tuberoso *et al*., 2014).

The addition of plasticizers to the orodispersible films increased the elongation at break (Gly>PEG>PP), confirming the greater plasticizer power of Gly observed in studies with DSC (*Tg* reduction) and FTIR, where both the plasticizers (Gly and PEG) affected the polymer matrix more intensely than PP and, therefore, contributed to higher values of elongation at break. In parallel, the low interaction between PP and the polymer matrix was responsible for the higher puncture strength values.

Oral mucosal adhesion is a specific term used to describe the interaction between the oral mucosa and the polymer matrix. Important variables in this process are the diffusion coefficient of the polymer in the mucin layer and the contact time between the polymer and the mucosa (Morales, McConville 2011).

In the adhesion test, the two-level interaction model (linear, linear) was the most appropriate for all the parameters assessed. For the parameter hardness (R-sqr = 0.95952; Adj:0.89206), the variables–polymer (linear) and plasticizer (linear, quadratic)–had a significant effect ($p < 0.05$); for the variable polymer, higher hardness was observed for the lower concentration (2%), regardless of the plasticizer type, and for the variable plasticizer, the hardness varied in the following order PP>PEG>Gly; for the parameter adhesiveness (R-sqr = 0.83991; Adj:0.57308), only the variable plasticizer (linear) presented a significant effect ($p < 0.05$) (Table III, Figure 4), and varied in the following order: Gly>PP>PEG; and finally, the parameter adhesive force (R-sqr = 0.62494; Adj:0.0000) was not influenced by the variables.

Optical properties

The Commission International de I'Eclairage, International Commission on Illumination (CIE) defines the color spaces in CIE *XYZ*, CIE *L*a*b** and CIE *L*C*h* using chromatic coordinates. Currently, color space *L*C*h* is preferred by some industry professionals because it correlates best with how the human eye perceives color.

Transparent films are characterized by low opacity (Santana *et al*., 2018). The opacity of the orodispersible films was calculated using the CIE XYZ color space and evaluated using DoE. The two-level interaction model (linear, linear) was the most appropriate (R-sqr = 0.95084; Adj:0.8689), and only the plasticizer (linear and quadratic) showed a significant effect ($p < 0.05$). Orodispersible films prepared with Gly and PP were similar, with greater transparency than those prepared with PEG.

Figure 4 shows the projections of the CIE *L*C*h* coordinates represented in a two-dimensional space, formed by the principal components, lightness (*L**, 27,60%), and chroma (*C**, 27.60%), which explained 96.71% of the data. The grouping of the samples, orodispersible films (F1-9), and standard polystyrene film (SD), into distinct quadrants indicated color differences between them. Samples F1, F4, and F5 presented the greatest transparency and similarity with SDs.

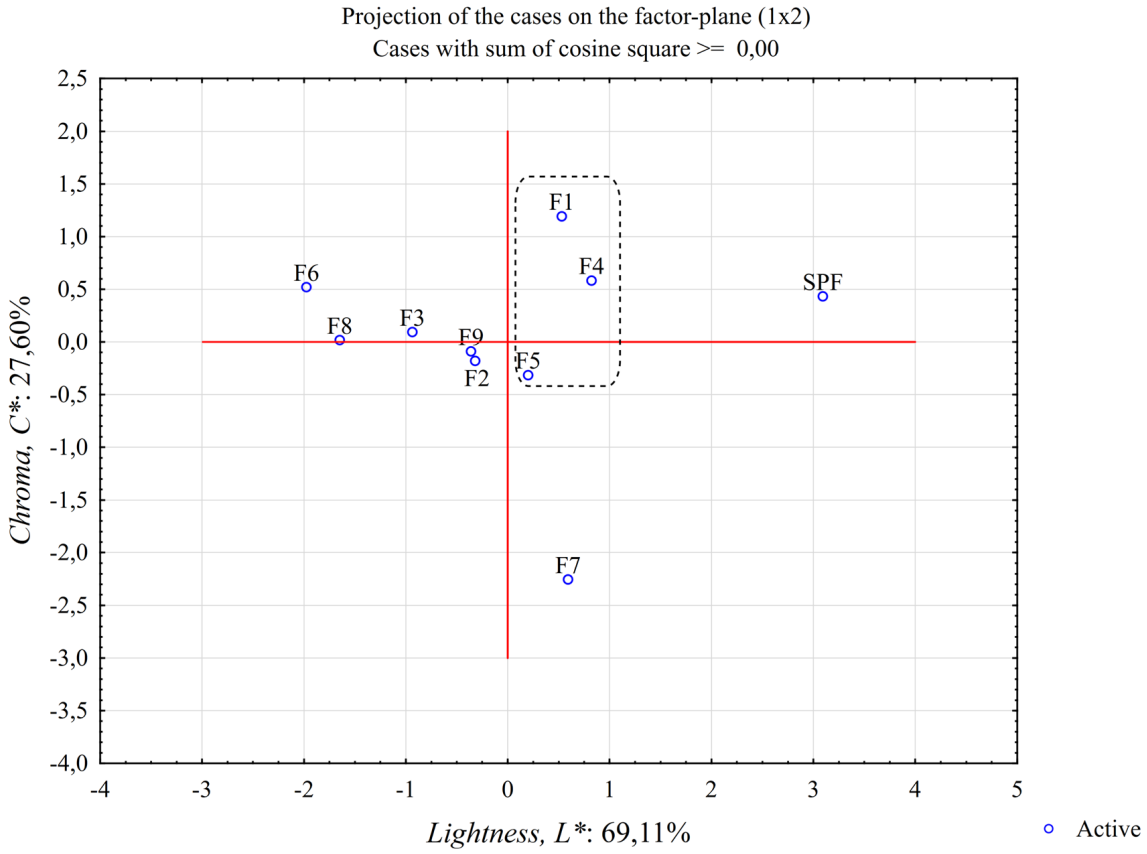

FIGURE 4 – Two-dimensional (2D) principal component analysis (PCA) score plot based on CIE *L*C*h* color coordinates.

SEM

The photomicrographs obtained by SEM for orodispersible films prepared with Gly or PEG showed the presence of fat droplets dispersed in these systems, suggesting greater difficulty in dispersing these plasticizers, whereas the orodispersible films prepared with PP showed a homogeneous surface (Figure 5).

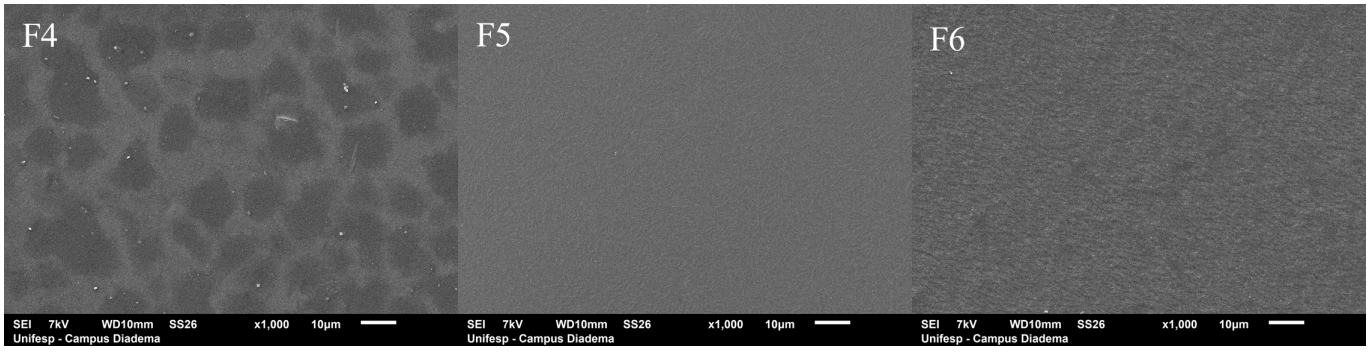

FIGURE 5 - Photomicrographs of orodispersible films obtained using scanning electron microscopy (SEM) Jeol with an increase of 1,000x.

Dissolution profile

Orodispersible films prepared with 3% polymer, Gly (F7), or PEG (F9) as a plasticizer, showed a lower dissolution rate of DOX, indicating that the amount of polymer and nature of the plasticizer may influence the release of drugs in orodispersible films. The dissolution profiles of the other orodispersible films were similar and lower than those of the reference product, Cardura™ 2 mg tablets (Pfizer Inc., Brazil) (Figure 6).

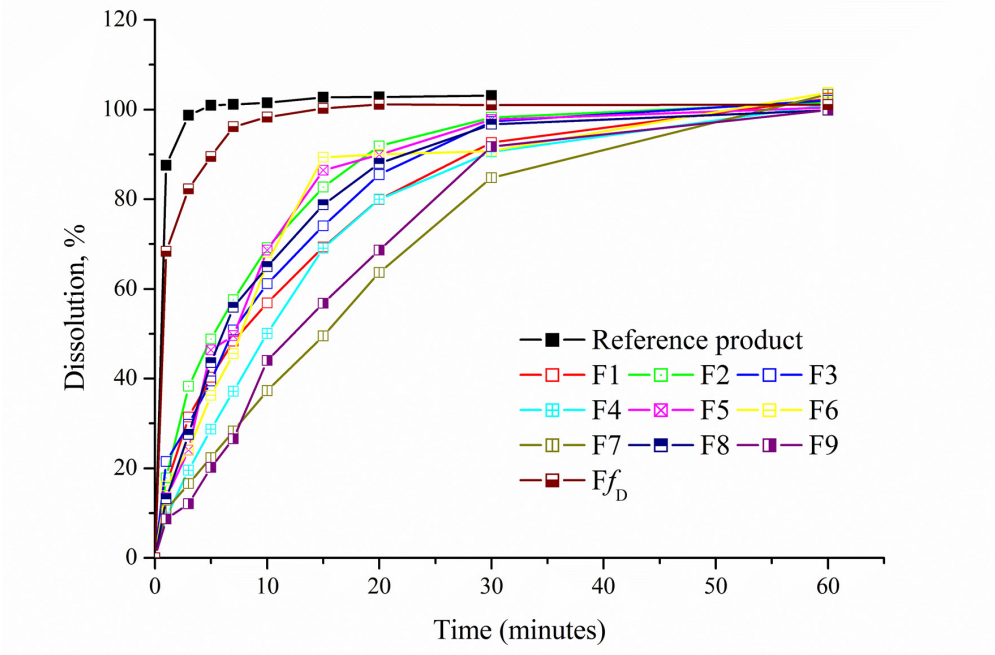

FIGURE 6 - Dissolution profiles of orodispersible films (F1-9) and the reference product (Cardura™ 2 mg tablets; Pfizer Inc., Brazil).

Dissolution efficiency (DE) is a parameter used to compare dissolution profiles and may correlate with *in vivo* data (Simionato *et al.*, 2018). The two-level interaction model (linear, linear) was the most appropriate (R-sqr=0.89993; Adj:0.73315), and the factors–polymer (linear) and plasticizer (quadratic)–showed a significant effect ($p < 0.05$). The dissolution efficiency decreased as a function of the amount of polymer, and the plasticizer effect followed the following proportions: PP>PEG>Gly (Table III, Figure 3).

In recent years, industries have successfully applied experimental planning to improve production efficiency and reduce processing costs without sacrificing the quality of their products (Farooq *et al.*, 2016). According to Goethals and Cho (2012), one of the main difficulties in solving problems of multiple characteristics (multivariate) is to optimize each of their characteristics simultaneously, and one of the most widely used methods to solve problems of multiple response optimization is the *desirability function*.

From the estimation of the effects obtained for the thickness, mechanical properties (elongation at break and adhesiveness), and DE of the films, it was possible to select the best formulation based on the desirability function (f_D) ($0 \leq f_D \leq 1$), using all factors in their optimal values (Figure 7). The maximum value for the desirability function (f_D) was 0.8668, corresponding to the use of 2.0–2.5% polymer (HPMC E6), and PP as a plasticizer.

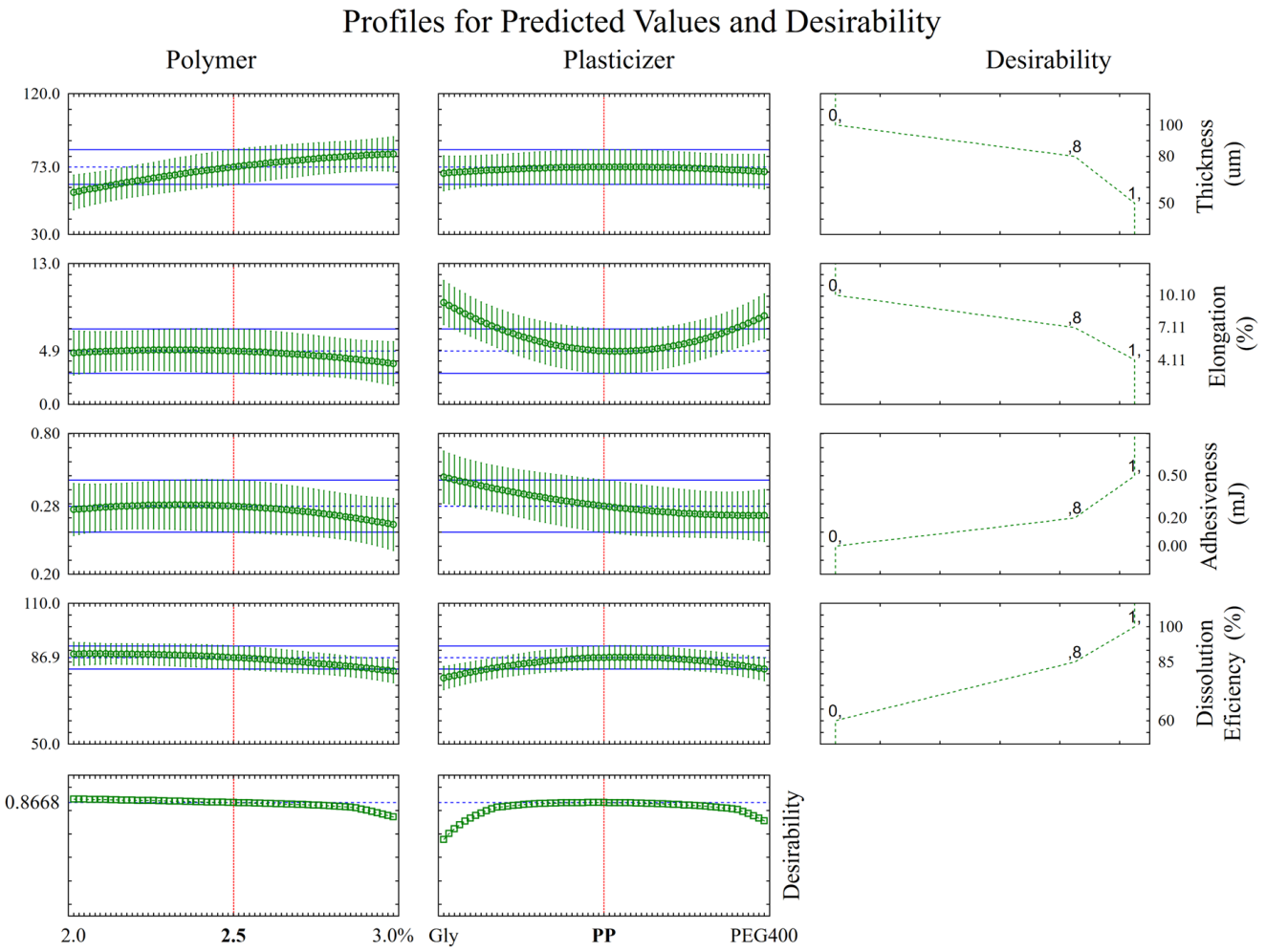

FIGURE 7 - Global desirability function (f_D= 0.8668).

DOX is a weak base salt (pk_{a1} = 12.67 e pk_{a2} = 7.24), and its bioavailability is strongly dependent on pH (Vincent *et al.*, 1983). Cha *et al.* (2010) suggested adding citric acid (1.7%) in oral dosage forms to increase the solubility and dissolution of DOX. In parallel, organic acids (citric acid, malic acid, ascorbic acid, tartaric acid, etc.) are saliva-stimulating agents that favor fast disintegration and dissolution of DOX in orodispersible films (Chonkar, Bhagawati, Udupa, 2015).

Based on these findings, a formulation consisting of 2.5% polymer (HPMC E6), PP (10% of the polymer amount), and 1.7% citric acid monohydrate was prepared, and named desirability formulation (F_D), and its dissolution profile compared to the reference product (Cardura™ 2 mg tablets, Pfizer Inc., Brazil) using the difference factor (f_1) and similarity factor (f_2) (Figure 6) (Xie, Ji, Cheng, 2015). The difference factor (f_1 = 6.84) and the similarity factor (f_2 = 52.07) indicated that the dissolution profiles of the dosage forms were similar.

pH and water activity are related to microbial growth, enzymatic activity, and product stability. According to Carvalho *et al.* (2010), pH 4.5 is the critical value for microbial growth; lower values inhibit microbial growth, while higher values favor the growth of bacteria, yeasts, and mold. Water activity (A_w) values range from 0 to 1.0, and in general, the A_w higher of a material, the higher the risk of microbial growth and degradation (Beuchat, 1982). All orodispersible films (F1-9) showed pH and water activity (A_w) values (Table III) higher than optimal conditions to inhibit microbial growth; therefore, the use

of preservatives is recommended. However, the addition of citric acid reduced the pH (pH ≅ 4.17) of the desirability formulation (F_D), favoring its biological stability.

CONCLUSION

In this study, an orodispersible film of DOX was successfully developed. Plasticizers play a critical role in the mechanical, optical, and dissolution properties of orodispersible films. DSC curves and XRPD diffractograms showed DOX amorphization, probably due to complexation with the polymer, HPMC E6, and the glass transition temperature of the polymer was reduced by adding a plasticizer in the order Gly>PP>PEG, which showed the best plasticizing power of Gly. These data agree with the results obtained in the elongation at break and adhesion tests, where Gly showed the best performance.

FTIR results showed that the chemical structure of DOX was preserved when introduced into the polymer matrix. PP was the plasticizer that produced the least alteration in the polymer matrix structure, reflecting the higher stiffness and lower elasticity of the films. Gly and PEG affected the polymer matrix with greater intensity, with greater elongation at break and dissolution rate of DOX in the films prepared with these plasticizers. The amorphous structure of the matrix was maintained by the addition of plasticizers and DOX.

Greater transparency and less opacity were observed for orodispersible films prepared with PP.

The addition of citric acid as a pH modifier is fundamental for the release of DOX. The desirability formulation (F_D) had its release profile similar to that of the reference product, indicating that this release system is promising as an alternative pharmaceutical form to the oral release of DOX.

ACKNOWLEDGMENTS

The authors would like to thank the Center for Technical Support for Teaching and Research (NATEP) and the Center for Research and Teaching Instrumentation for XRDP analysis; and the Laboratory of Hybrid Materials (LMH) for the use of FTIR-ATR.

REFERENCES

Altiokka G. Voltammetric determination of doxazosin in tablets using rotating platinum electrode. J Pharm Biomed Anal. 2001;25(3-4):387-91.

ASTM D2582 - 16. In: Standard Test Method for Puncture-Propagation Tear Resistance of Plastic Film and Thin Sheeting [Internet]. Available from: https://www.astm.org/Standards/D2582.htm

ASTM D4541 - 17. In: Standard Test Method For Pull-Off Strength Of Coatings Using Portable Adhesion Testers [Internet]. Available from: https://www.astm.org/Standards/D4541.htm

ASTM D6132-13(2017). In: Standard Test Method for Nondestructive Measurement of Dry Film Thickness of Applied Organic Coatings Using an Ultrasonic Coating Thickness Gage [Internet]. Available from: https://www.astm.org/Standards/D6132.htm

Beuchat LR. Thermal Inactivation of Yeasts in Fruit Juices Supplemented with Food Preservatives and Sucrose. J Food Sci. 1982;47(5):1679-82.

Bharti K, Mittal P, Mishra B. Formulation and characterization of fast dissolving oral films containing buspirone hydrochloride nanoparticles using design of experiment. J Drug Deliv Sci Technol. 2019;49:420-32.

Biswas N, Guha A, Sahoo RK, Kuotsu K. Pulse release of doxazosin from hydroxyethylcellulose compression coated tablet: Mechanistic and in vivo study. Int J Biol Macromol. 2015;72:537-43.

Borges AF, Silva C, Coelho JFJJ, Simões S. Oral films: Current status and future perspectives: I-Galenical development and quality attributes. J Control Release 2015;28(206):1-19.

Candioti LV, de Zan MM, Cámara MS, Goicoechea HC. Experimental design and multiple response optimization. Using the desirability function in analytical methods development. Talanta. 2014;124:123-38.

Carvalho FC, Bruschi ML, Evangelista RC, Gremião MPD. Mucoadhesive drug delivery systems. Braz J Pharm Sci. 2010;46(1):1-17.

Cha KH, Tran TH, Kim MS, Kim JS, Park HJ, Park J, *et al.* PH-independent sustained release matrix tablet containing doxazosin mesylate: Effect of citric acid. Arch Pharm Res. 2010;33(12):2003-9.

Chauhan K, Solanki R, Sharma S. A review on fast dissolving tablet. Int J Appl Pharm. 2018;10(6):1-7.

Chonkar AD, Bhagawati ST, Udupa N. An Overview on Fast Dissolving Oral Films. Asian J Pharm Technol. 2015;5(3):129-37.

Coelho BP, Gaelzer MM, dos Santos Petry F, Hoppe JB, Trindade VMT, Salbego CG, *et al.* Dual Effect of Doxazosin: Anticancer Activity on SH-SY5Y Neuroblastoma Cells and Neuroprotection on an In Vitro Model of Alzheimer's Disease. Neurosci. 2019;404:314-32

Dedroog S, Pas T, Vergauwen B, Huygens C, Van den Mooter G. Solid-state analysis of amorphous solid dispersions: Why DSC and XRPD may not be regarded as stand-alone techniques. J Pharm Biomed Anal. 2020;178:112937.

Dinge A, Nagarsenker M. Formulation and evaluation of fast dissolving films for delivery of triclosan to the oral cavity. AAPS PharmSciTech. 2008;9(2):349-56.

Dixit RP, Puthli SP. Oral strip technology: Overview and future potential. J Control Release. 2009;139(2):94-107.

Farooq MA, Nóvoa H, Araújo A, Tavares SMOO. An innovative approach for planning and execution of pre-experimental runs for Design of Experiments. Eur Res Manag Bus Econ. 2016;22(3):155-61.

Faulkner JK, Himanen P, Karjalainen U, Saraste M. The pharmacokinetics and pharmacodynamics of doxazosin compared with atenolol during long-term double-blind treatment. Eur J Clin Pharmacol. 1987;31(6):685-93.

Gittings S, Turnbull N, Henry B, Roberts CJ, Gershkovich P. Characterisation of human saliva as a platform for oral dissolution medium development. Eur J Pharm Biopharm. 2015;91:16-24.

Goethals PL, Cho BR. Extending the Desirability Function to Account for Variability Measures in Univariate and Multivariate Response Experiments. Comput Ind Eng. 2012;62(2):457-68.

Grčman M, Vrečer F, Meden A. Some physico-chemical properties of doxazosin mesylate polymorphic forms and its amorphous state. J Therm Anal Calorim. 2002;68(2):373-87.

Hazzah HA, EL-Massik MA, Abdallah OY, Abdelkader H. Preparation and characterization of controlled-release doxazosin mesylate pellets using a simple drug layering-aquacoating technique. J Pharm Investig. 2013;43(4):333-42.

Karki S, Kim H, Na S-JJ, Shin D, Jo K, Lee J. Thin films as an emerging platform for drug delivery. Asian J Pharm Sci. 2016;11(5):559-74.

Khalilullah H, Khan S, Nomani MS, Ahmed B. Synthesis, characterization and antimicrobial activity of benzodioxane ring containing 1,3,4-oxadiazole derivatives. Arab J Chem. 2016;9(Suppl 2):S1029-S1035.

Krampe R, Sieber D, Pein-Hackelbusch M, Breitkreutz J. A new biorelevant dissolution method for orodispersible films. Eur J Pharm Biopharm. 2016;98:20-5.

Mahadevaiah, Shivakumara LR, Demappa T, Vasudev S. Mechanical and Barrier Properties of Hydroxy Propyl Methyl Cellulose Edible Polymer Films with Plasticizer Combinations. J Food Process Preserv. 2017;41(4):1-10.

Morales JO, McConville JT. Manufacture and characterization of mucoadhesive buccal films. Eur J Pharm Biopharm. 2011;77(2):187-99.

Munjal B, Suryanarayanan R. Applications of synchrotron powder X-ray diffractometry in drug substance and drug product characterization. TrAC Trends Anal Chem. 2021;136:116181.

Musazzi UM, Khalid GM, Selmin F, Minghetti P, Cilurzo F. Trends in the production methods of orodispersible films. Int J Pharm. 2020;576:118963.

Preis M, Knop K, Breitkreutz J. Mechanical strength test for orodispersible and buccal films. Int J Pharm. 2014;461(1-2):22-9.

Pupe CG, do Carmo FA, de Sousa VP, Lopes M, Abrahim-Vieira B, Ribeiro AJ, *et al.* Development of a doxazosin and finasteride transdermal system for combination therapy of benign prostatic hyperplasia. J Pharm Sci. 2013;102(11):4057-64.

Radebaugh GW, Murtha JL, Julian TN, Bondi JN. Methods for evaluating the puncture and shear properties of pharmaceutical polymeric films. Int J Pharm. 1988;45(1-2):39-46.

Ramaraj B, Nayak SK, Yoon KR J. Poly(vinyl alcohol) and layered double hydroxide composites: Thermal and mechanical properties. Appl Polym Sci. 2010;116(3):1671-77.

Rani NS, Sannappa J, Demappa T, Mahadevaiah. Structural and ionic conductivity behavior in hydroxypropylmethylcellulose (HPMC) polymer films complexed with sodium iodide (NaI). AIP Conference Proceedings. 2013;1512(1):544-545.

Rowe RR, Sheskey PJ, Quinn ME. Handbook of Pharmaceutical Excipients. Sixth Edition. Revue des Nouvelles Technologies de l'Information. 2015.

Santana RF, Bonomo RCF, Gandolfi ORR, Rodrigues LB, Santos LS, dos Santos Pires AC, *et al.* Characterization of starch-based bioplastics from jackfruit seed plasticized with glycerol. J Food Sci Technol. 2018;55(1):278-86.

Siddiqui MDN, Garg F, Sharma PK. A Short Review on "A Novel Approach in Oral Fast Dissolving Drug Delivery System and Their Patents." Adv Biol Res. 2011;5(6):291-303.

Simionato LD, Petrone L, Baldut M, Bonafede SL, Segall AI. Comparison between the dissolution profiles of nine meloxicam tablet brands commercially available in Buenos Aires, Argentina. Saudi Pharm J. 2018;26(4):578-84.

Tuberoso CIG, Jerković I, Sarais G, Congiu F, Marijanović Z, Kuś PM. Color evaluation of seventeen European unifloral honey types by means of spectrophotometrically determined CIE-L*Cab*h(ab)° chromaticity coordinates. Food Chem. 2014;145:284-91.

Uhoraningoga A, Kinsella GK, Henehan GT, Ryan BJ. The goldilocks approach: A review of employing design of experiments in prokaryotic recombinant protein production. Bioengineering. 2018;5(89):1-27.

USP. U.S. Pharmacopoeia-National Formulary [USP 38 NF 33]. In: Rockville, Md: United States Pharmacopeial Convention. 2015.

Usui F, Maeda K, Kusai A, Nishimura K, Yamamoto K. Inhibitory effects of water-soluble polymers on precipitation of RS-8359. Int J Pharm. 1997;154(1):59-66.

Veiga F, Pecorelii C, Ribeiro LF, Pecorelii C, Ribeiro L. As Ciclodextrinas em Tecnologia Farmacêutica. 1ª ed. MinervaCoimbra, editor. Coimbra; 2006.

Vincent J, Elliott H, Meredith P, Reid J. Doxazosin, an alpha 1-adrenoceptor antagonist: pharmacokinetics and concentration-effect relationships in man. Br J Clin Pharmacol. 1983;15(6):719-25.

Van Der Weerd J, Kazarian SG. Combined approach of FTIR imaging and conventional dissolution tests applied to drug release. J Control Release. 2004;98(2):295-305.

Wray PS, Clarke GS, Kazarian SG. Application of FTIR spectroscopic imaging to study the effects of modifying the pH microenvironment on the dissolution of ibuprofen from HPMC matrices. J Pharm Sci. 2011;100(11):4745-755.

Xie F, Ji S, Cheng Z. In vitro dissolution similarity factor (f2) and in vivo bioequivalence criteria, how and when do they match? Using a BCS class II drug as a simulation example. Eur J Pharm Sci. 2015;66:163-72.

Received for publication on 19th February 2021
Accepted for publication on 19th September 2021